RAA 2016 Vol. **16** No. **4**, 58 (8pp) doi: 10.1088/1674–4527/16/4/058
http://www.raa-journal.org *http://iopscience.iop.org/raa*

***R**esearch in*
***A**stronomy and*
***A**strophysics*

Detecting the errors in solar system ephemeris by pulsar timing

Liang Li[1,2], Li Guo[1] and Guang-Li Wang[1]

[1] Shanghai Astronomical Observatory, Chinese Academy of Sciences, Shanghai 200030, China; *lli@shao.ac.cn*
[2] University of Chinese Academy of Sciences, Beijing 100049, China

Received 2015 June 17; accepted 2015 November 1

Abstract Pulsar timing uses planetary ephemerides to convert the measured pulse arrival time at an observatory to the arrival time at the Solar System barycenter (SSB). Since these planetary ephemerides cannot be perfect, a method of detecting the associated errors based on a pulsar timing array is developed. By using observations made by an array of 18 millisecond pulsars from the Parkes Pulsar Timing Array, we estimated the vector uncertainty from the Earth to the SSB of JPL DE421, which reflects the offset of the ephemeris origin with respect to the ideal SSB, in different piecewise intervals of pulsar timing data, and found consistent results. To investigate the stability and reliability of our method, we divided all the pulsars into two groups. Both groups yield largely consistent results, and the uncertainty of the Earth-SSB vector is several hundred meters, which is consistent with the accuracy of JPL DE421. As an improvement in the observational accuracy, pulsar timing will be helpful to improve the solar system ephemeris in the future.

Key words: astrometry — ephemerides — pulsars: general

1 INTRODUCTION

High precision planetary ephemerides are widely used in planetary exploration, deep space navigation and many astronomical applications. Since the 1980s, NASA's Jet Propulsion Laboratory has released the Development Ephemeris (DE) series of ephemerides (Standish 1982), and many other ephemerides have become available, such as the INPOP series of numerical ephemerides (Fienga et al. 2008) developed at the IMCCE-Observatoire de Paris and the EPM ephemerides (Pitjeva 2009) of IAA RAS. Purple Mountain Observatory has also developed the PMOE ephemeris (Li et al. 2003) primarily for the project Astro-dynamical Space Test of Relativity using Optical Devices (Mini-ASTROD). All of these ephemerides are computed from the simultaneous numerical integration of dynamical models of major solar system objects and provide users positions and velocities of planets at a given time.

The origin of the celestial reference frame in planetary ephemerides is at the solar system barycenter (SSB). The values of planetary mass for the constructed ephemerides will directly affect the computed position of the SSB. Due to the limited accuracy of the measured mass and other unknown masses in the solar system, the origin of the ephemerides frame is offset with respect to the ideal SSB, which is defined as the center of the mass distribution of all bodies in the solar system. The offset has an effect on the vector from the Earth to the SSB in the ephemerides. Many applications of planetary ephemerides are not critical to the SSB position, but pulsar timing is directly related to the positional accuracy of the SSB. Hence, pulsar timing arrays can provide an independent method to study shifts in the computed SSB position.

In the technique of pulsar timing, times of arrival (ToAs) of pulses measured at an observatory are converted to the SSB by using a planetary ephemeris. The differences between the computed arrival time and the theoretical arrival time that is predicted by pulsar timing models are known as "timing residuals." If the position of the SSB in the ephemerides is shifted, it will introduce a dipolar perturbation into the timing residuals. Previous work to measure the planetary mass by a pulsar timing array has been done by Champion et al. (2010). They assumed the position shift of the SSB is caused by the mass error of some planets,

$$\Delta \boldsymbol{r}^{\rm ssb} = \sum_j \boldsymbol{r}_j \frac{\Delta M_j}{M_T}\,, \qquad (1)$$

where ΔM_j is the mass error, M_T is the sum of mass in the solar system and $\boldsymbol{r}_j$ is the vector position of the object. By using four pulsars, the masses of the planetary systems from Mercury to Saturn have been determined with uncertainties larger than the planetary masses obtained from direct spacecraft exploration. Errors in planetary ephemerides add systematic noise to the timing residuals for different pulsars that are partially correlated among pulsars. Based on the mathematical relation between the vector errors from the Earth to the SSB and the timing residuals, we developed a method to estimate those errors by a pulsar timing array.

In Section 2 we describe the timing model and analyze the effects of the Earth-SSB vector uncertainty on pulsar

timing residuals. The observations are described and residual plots in our sample are presented in Section 3. Section 4 describes data analysis methods and summarizes the results. The conclusion is presented in Section 5.

2 ANALYSIS

We can briefly express the measured pulse arrival time (site arrival time, sat) of the observation number n of the $i^{\rm th}$ pulsar at an observatory as follows

$$\begin{aligned} {}^{\rm sat}t_i^n &= {}^{\rm emi}t_i^0 + \Delta^{\rm geo}t_i^0 + \Delta^{\rm int}t_i^n + {}^{\rm BS}t_i^n \\ &\quad -(\Delta^{\rm geo}t_i^n + {}^{\rm phy}t_i^n) + \epsilon_i^n \,, \end{aligned} \tag{2}$$

where ${}^{\rm emi}t_i^0$ is the reference pulse emission time (a reference time) at the pulsar. $\Delta^{\rm geo}t_i^0$ is the vacuum propagation delay from the pulsar barycenter (barycenter of the binary system in the case of a binary pulsar) to the SSB. $\Delta^{\rm int}t_i^n$ is the time interval between the expected pulse number n and the reference pulse. ${}^{\rm BS}t_i^n$ is the binary orbital delay due to the presence of a binary companion in the case of a binary system. $\Delta^{\rm geo}t_i^n$ is the vacuum geometric propagation delay due to motion of the observatory around the SSB. ${}^{\rm phy}t_i^n$ is the sum of delays owing to physical factors, such as clock corrections, Einstein delays, atmospheric delays, Shapiro delays, interstellar propagation delays and so on. ϵ_i^n is the measurement error. As the periodicity of the pulses is extremely stable, the sum of the first three terms in Equation (2) is expressed by the timing models. So, the predicted SSB arrival time of the expected pulse number n, ${}^{\rm bat}t_i^n$, is expressed in the following form if we only account for terms that take the form of quadratic polynomials in the timing model

$${}^{\rm bat}t_i^n = {}^{\rm bat}t_i^0 + P_0 n + \frac{1}{2}P_1 n^2 + {}^{\rm BS}t_i^n \,, \tag{3}$$

where ${}^{\rm bat}t_i^0$ is the reference time, and P_0 and P_1 are the period and the time derivative of period of the pulsar at SSB respectively. The binary orbital delay ${}^{\rm BS}t_i^n$ will be zero if it is a single pulsar. Eventually, as we showed in Equation (3), Equation (2) can be rewritten

$$\begin{aligned} {}^{\rm sat}t_i^n &= {}^{\rm bat}t_i^0 + P_0 n + \frac{1}{2}P_1 n^2 + {}^{\rm BS}t_i^n \\ &\quad -(\Delta^{\rm geo}t_i^n + {}^{\rm phy}t_i^n) + \epsilon_i^n \,. \end{aligned} \tag{4}$$

The differences between observed and calculated values of ${}^{\rm sat}t_i^n$ are known as timing residuals. Errors in the timing parameters will introduce a systematic trend in the timing residuals. According to Equation (4), then expanding the $\Delta^{\rm geo}t_i^n$, the timing residuals are denoted as follows

$$\begin{aligned} \delta t_i^n &= \Delta P_0 n + \frac{1}{2}\Delta P_1 n^2 + \Delta^{\rm BS}t_i^n - \Delta^{\rm phy}t_i^n \\ &\quad + \epsilon_i^n - \frac{1}{c}\boldsymbol{k}_i \cdot \Delta\boldsymbol{r}_{\rm o}^{\rm ssb} - \frac{1}{c}(\Delta\boldsymbol{k}_i \cdot \boldsymbol{r}_{\rm o}^{\rm ssb}) \\ &\quad + \frac{1}{c}\boldsymbol{k}_i \cdot \Delta{\boldsymbol{v}_i}^{\parallel}\Delta t^n - \frac{1}{c}\Delta\boldsymbol{\mu}_i \cdot \boldsymbol{r}_{\rm o}^{\rm ssb}\Delta t^n \\ &\quad + \frac{\Delta\rho_i}{2c}|\boldsymbol{k}_i \times \boldsymbol{r}_{\rm o}^{\rm ssb}|^2 \,, \end{aligned} \tag{5}$$

where ΔP_0 and ΔP_1 are the uncertainty in the period and its rate of change respectively. $\Delta^{\rm BS}t_i^n$ is the model error associated with a binary orbit. $\Delta^{\rm phy}t_i^n$ is the uncertainty in delays due to physical effects. c is the vacuum speed of light, $\boldsymbol{k}_i$ is the unit position vector of the $i^{\rm th}$ pulsar at the reference time, $\boldsymbol{r}_{\rm o}^{\rm ssb}$ is the barycentric position of the observatory and $\Delta\boldsymbol{r}_{\rm o}^{\rm ssb}$ is the uncertainty in the vector from the observatory to the SSB. $-\frac{1}{c}\boldsymbol{k}_i\cdot\Delta\boldsymbol{r}_{\rm o}^{\rm ssb}$ is the term representing the effect that the uncertainty has on pulse arrival time. $-\frac{1}{c}(\Delta\boldsymbol{k}_i \cdot \boldsymbol{r}_{\rm o}^{\rm ssb})$ is the influence of the unit position vector error associated with the pulsar. The form of the residual will be revealed by an annual trend in the timing residuals. $\frac{1}{c}\boldsymbol{k}_i \cdot \Delta{\boldsymbol{v}_i}^{\parallel}\Delta t^n$ represents variations due to radial motion ($\boldsymbol{k}_i \cdot \Delta\boldsymbol{v}_i^{\parallel}$), which cannot be distinguished from the period of the pulsar. $-\frac{1}{c}\Delta\boldsymbol{\mu}_i\cdot\boldsymbol{r}_{\rm e}^{\rm ssb}\Delta t^n$ is the annual proper motion term. $\frac{\Delta\rho_i}{2c}|\boldsymbol{k}_i \times \boldsymbol{r}_{\rm e}^{\rm ssb}|$ is the parallax term.

A summary of the timing effects is presented in Table 1. For further details refer to Edwards et al. (2006). The fifth column describes whether the term generates systematic signals among pulsars. In the process of obtaining timing solutions, the position vector error ($\Delta\boldsymbol{k}_i$), annual proper motion error ($\Delta\boldsymbol{\mu}_i$), parallax error ($\Delta\rho_i$), the parameters describing a binary orbit, and the spin parameters will be involved in the adjustment to minimize the timing residuals with a least-squares fitting procedure, and we ignore the geocentric position error of the observatory due to its accuracy of several mm in position (Schuh & Behrend 2012).

According to Table 1, the errors arising from interstellar propagation delays are uncorrelated between different pulsars. Assuming that the errors from physical effects and astrometric errors except for $\Delta\boldsymbol{r}_{\rm o}^{\rm ssb}$ are negligible after appropriate processing, the timing residuals for a pulsar timing array are simplified as follows

$$\delta t_i^n = -\frac{1}{c}\boldsymbol{k}_i \cdot \Delta\boldsymbol{r}_{\rm e}^{\rm ssb} + \epsilon_i^n \,, \tag{6}$$

where $\Delta\boldsymbol{r}_{\rm e}^{\rm ssb}$ is the uncertainty in the vector from the Earth to the SSB, which can be expressed in the form

$$\begin{aligned} \Delta\boldsymbol{r}_{\rm e}^{\rm ssb} &= \Delta\boldsymbol{r}_{\rm e}^{\rm sun} + \Delta\boldsymbol{r}_{\rm sun}^{\rm ssb} \\ &= \Delta\boldsymbol{r}_{\rm e}^{\rm sun} + \Delta\boldsymbol{r}_0^{\rm ssb} + \Delta\dot{\boldsymbol{r}}^{\rm ssb}\Delta t \\ &\quad + \frac{1}{2}\Delta\ddot{\boldsymbol{r}}^{\rm ssb}\Delta t^2 + \delta\boldsymbol{r}^{\rm ssb} \,, \end{aligned} \tag{7}$$

where $\Delta\boldsymbol{r}_{\rm e}^{\rm sun}$ is the uncertainty in the vector from the Earth to the Sun. It appears as an annual sinusoid and will be absorbed in the fitted pulsar position $\boldsymbol{k}_i$. $\Delta\boldsymbol{r}_{\rm sun}^{\rm ssb}$ is the uncertainty in the vector from the Sun to the SSB, which is a secular term and can be rewritten as the sum of a quadratic polynomial term and the remaining term ($\delta\boldsymbol{r}^{\rm ssb}$). $\Delta\boldsymbol{r}_0^{\rm ssb}$ is the position offset between the origin in the ephemeris and the ideal SSB at the reference time, $\Delta\dot{\boldsymbol{r}}^{\rm ssb}$ and $\Delta\ddot{\boldsymbol{r}}^{\rm ssb}$ are the relative velocity and acceleration between the origin and the ideal SSB respectively.

In Figure 1 we compare the heliocentric and barycentric range of Earth between different ephemerides. The difference in the barycentric range is significantly greater than

Table 1 Terms in the Timing Model

Term	Trends in Residuals	Accuracy Estimates	Adjustment	PSR-PSR Correlation
ΔP_0	Linear Trend	-	Y	N
ΔP_1	Parabolic Trend	-	Y	N
Binary Parameters	-	-	Y	N
Clock Corrections	-	$\sim$10 ns[1]	N	Correlated
Atmospheric Delays	-	$<$10 ns[1]	N	N
Einstein Delays	-	100 ps[1]	N	-
Shapiro Delays	-	0.5 ns[1]	N	-
Interstellar Propagation Delays	-	$\sim$100 ns[1]	N	N
$\Delta \boldsymbol{r}_{\rm o}^{\rm ssb}$	-	$\sim$ 1 μs[2]	N	Partially Correlated
$\Delta \boldsymbol{k}_i$	Annual Trend	-	Y	N
$\Delta \boldsymbol{v}_i^{\parallel}$	Linear Trend	-	Y	N
$\Delta \boldsymbol{\mu}_i$	Annual Trend Change in Amplitude	-	Y	N
$\Delta \rho_i$	Semi-annual Trend	-	Y	N

Notes: [1] stands for Edwards et al. (2006) and references therein, and [2] stands for Folkner et al. (2009).

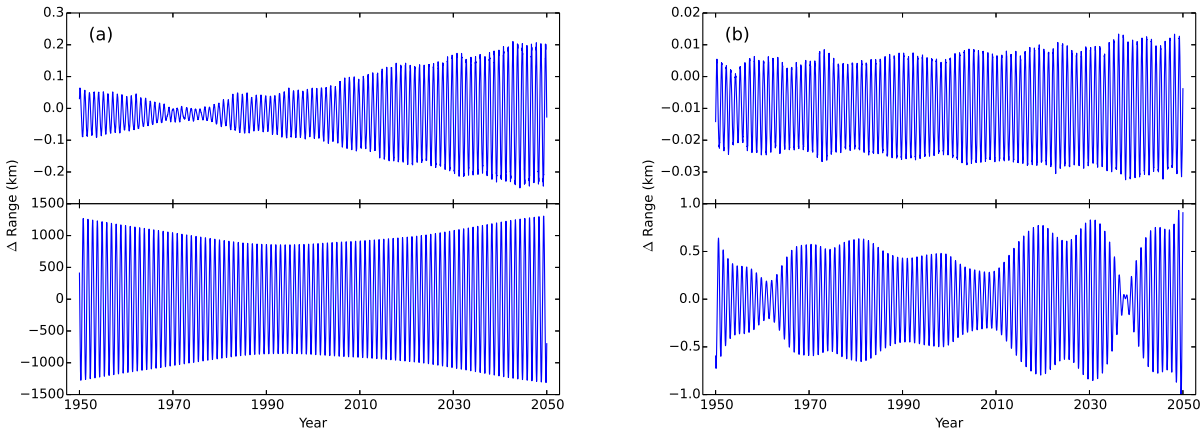

Fig. 1 The top panels show the difference in the heliocentric range of Earth for (a) DE200 and (b) DE405 with respect to DE421. The bottom panels show the difference in the barycentric range of Earth.

that in the heliocentric range, which indicates that $\Delta \boldsymbol{r}_{\rm sun}^{\rm ssb}$ is the main source of uncertainty in the Earth-SSB vector. Furthermore, $\Delta \boldsymbol{r}_{\rm e}^{\rm sun}$ and Δk_i are revealed by an annual trend in the timing residuals, and the quadratic polynomial term in $\Delta \boldsymbol{r}_{\rm sun}^{\rm ssb}$ has a correlation with the spin parameters. The quadratic term and the annual term are not detected in timing solutions, and that really reduces the sensitivity to the ephemeris errors. In general, we can only estimate $\delta \boldsymbol{r}^{\rm ssb}$ by a pulsar timing array owing to this correlation. $\delta \boldsymbol{r}^{\rm ssb}$ can reflect the offset in the origin of the ephemeris frame with respect to the ideal SSB to some extent, hereafter called the offset of the origin.

3 DATA SETS

The pulsar timing data used in this analysis include observations chosen from the Parkes Pulsar Timing Array (PPTA) project (Hobbs et al. 2010), and 18 Millisecond Pulsars (MSPs) with high accuracy in their ToAs were selected. The pulsar parameters were obtained from the ATNF Pulsar Catalogue (Manchester et al. 2005). The main aim of the project is detection of gravitational waves, and the pulsars used in that project have high observational accuracy and are distributed evenly across the celestial sphere. All the pulsars are observed with the Parkes 64-m radio telescope, and each observation of a pulsar is typically 1 hour in duration. The PPTA is a set of 20 pulsars, but we have not included PSR J1939+2134 or PSR J1824–2452A, as we noticed that there are some indications of low frequency noise in our data sets. All 18 MSPs have a similar data span of about 2004–2010. Detailed information about our data sets is provided in Table 2, where the columns present the pulsar name, the data span, the number of ToAs, the RMS timing residuals and the grouping of the pulsars in our analysis.

For each observation, the time of arrival was obtained by correlating a single pulse profile with a high signal-to-noise ratio template (the standard profile). The standard profile and the estimation of ToAs are obtained with the PSRCHIVE package (Hotan et al. 2004). The TEMPO2

Table 2 The Data Sets

PSRJ	MJD Range	$N_{\rm obs}$	RMS (μs)	Group
J0437–4715	53069–55344	637	0.639	A&B
J0613–0200	53087–55364	130	0.645	B
J0711–6830	53144–55345	103	1.658	A
J1022+1001	53082–55345	145	1.859	A&B
J1024–0719	53069–55326	89	3.798	A
J1045–4509	53070–55364	127	4.874	B
J1600–3053	53070–55364	273	1.051	A
J1603–7202	53070–55365	95	1.844	B
J1643–1224	53082–55364	111	2.08	A
J1713+0747	53070–55344	159	0.927	A&B
J1730–2304	53082–55364	85	2.542	B
J1732–5049	53070–55365	74	3.639	A
J1744–1134	53070–55365	181	0.995	B
J1857+0943	53086–55364	90	1.654	A&B
J1909–3744	53070–55365	398	0.702	A
J2124–3358	53069–55363	136	3.501	B
J2129–5721	53070–55363	69	2.677	A
J2145–0750	53069–55364	138	2.207	B

software package (Hobbs et al. 2006) is used to obtain the timing solution. The period and the first derivative of the period, but no higher order period parameters, were fitted in the data processing using TEMPO2 in our analysis. Timing residuals were calculated using the JPL DE421 and referred to TT(BIPM2011), and the timing residuals are shown in Figure 2.

4 METHOD AND RESULTS

To estimate the offset of the origin, we describe it as a set of equally spaced samples during the data span. The sampling interval is annual, semi-annual and quarterly. We use the least-squares procedure to estimate the offset for piecewise fitting of the timing residuals. In our analysis, we assume the χ^2 per degree of freedom of the fit is unity. We add the same amount of noise to each observation of a pulsar to bring the χ^2 per degree of freedom to unity.

In order to test our method, we applied it to the simulation of timing residuals for 18 MSPs. We generated the simulated observations using the TOASIM plugin package to TEMPO2 (Deng et al. 2013). Each pulsar has the same spin parameters, astrometric parameters and binary parameters as the real data sets. As with the actual observations, the simulated data are unevenly sampled and different ToAs have different uncertainties. Some unmodeled physics, such as pulsar rotation irregularities, variations in interstellar dispersion, gravitational waves, etc, will introduce red noise into the timing residuals. Coles et al. (2011) model the red noise spectrum in the form

$$P(f) = A[1 + (f/f_{\rm c})^2]^{-\alpha/2}\,, \tag{8}$$

where A is the strength of the red noise, $f_{\rm c}$ is a corner frequency and α is the spectral exponent of the red noise. We generated the additive red noise using the measured spectral parameters of the red noise for PPTA data sets. The values of A, $f_{\rm c}$ and α are obtained from Wang et al. (2015). Based on Equation (4), we calculated the vacuum geometric propagation delays using JPL DE421 solar system ephemeris and simulated the observations with the pulsar parameters. Actually, we assume that DE421 is perfect and the origin of DE421 is the ideal SSB. Then, we generated the timing residuals using the TEMPO2 software with DE200.

Finally we estimated the offset of the origin of DE200 relative to DE421. The result of our simulations is shown in Figure 3. The offset estimated with simulation data has the same features as the actual differences between DE421 and DE200. From the above analysis, the differences between DE421 and DE200 are included in the vector from the Sun to the SSB after a quadratic term has been removed. Large errors at the start and end time of the data span are mainly due to lack of observations for some certain pulsars.

Verbiest et al. (2008) demonstrated that the timing residuals of 20 MSPs in the PPTA project have unexplained low-frequency features. In the work done by Champion et al. (2010), the timing data were preprocessed and whitened. Currently, the treatment of low-frequency noise processes, such as Harmonic Whitening (Hobbs et al. 2004) and Cholesky Whitening (Coles et al. 2011), is only mathematical and does not have a coherent physical basis. As presented by Verbiest et al. (2009), there are three pulsars (PSRs J0613-0200, J1024-0719, J1045-4509) that show some low-frequency features, but at lower white noise levels. The remaining pulsars have no obvious low-frequency noise that prevents gravitational-wave background detection. In our data sets, there are no significant low-frequency features except PSR J1045-4509. According to Folkner et al. (2009), the orbit of Earth is known to sub-kilometer accuracy, which is approximately

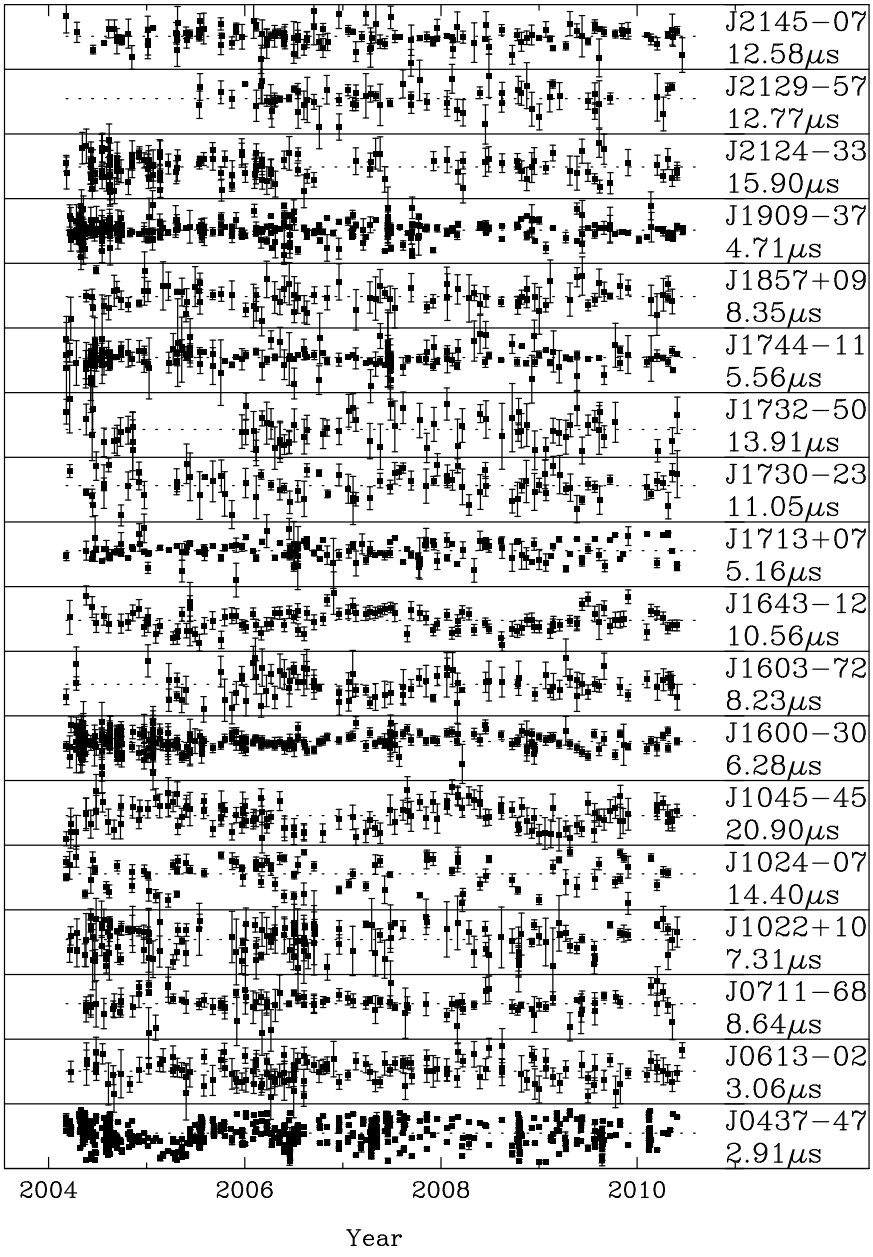

Fig. 2 The timing residuals of 18 MSPs. The pulsar name and the range of the residuals are given on the right.

on the same order as the low-frequency noise. Considering that the mathematical treatment of low-frequency noise processes would weaken the signal of the offset and the low-frequency noises of different pulsars have different features that will not introduce systematic effects into the result, we did not whiten the data.

The intrinsic variations of pulsars and variations in the interstellar propagation path are uncorrelated in residuals computed from a pulsar timing array. The gravitational waves have a quadrupolar effect with a very weak signal in the timing residuals, which will not have systematic effects on the offset. The stability of terrestrial time will affect the timing residuals. TT(TAI) is the realization of terrestrial time that is combined by the Bureau International des Poids et Mesures (BIPM), and TT(BIPM) is the revised and authorized confirmation. Hobbs et al. (2004) showed that the TT(BIPM) is adequate for current MSP timing experiments. The effects caused by the errors in terrestrial time are also neglected in our analysis. We estimated the offset of the origin in DE421 with different piecewise intervals, and the results are shown in Figure 4.

To investigate the stability and reliability of our method, we divided all the pulsars into two groups (A/B) according to the distributions of pulsars on the celestial sphere. For details about the grouping, refer to Figure 5 and Table 2. We estimated the offset with different groups using the same analysis process, and the result is presented in Figure 6.

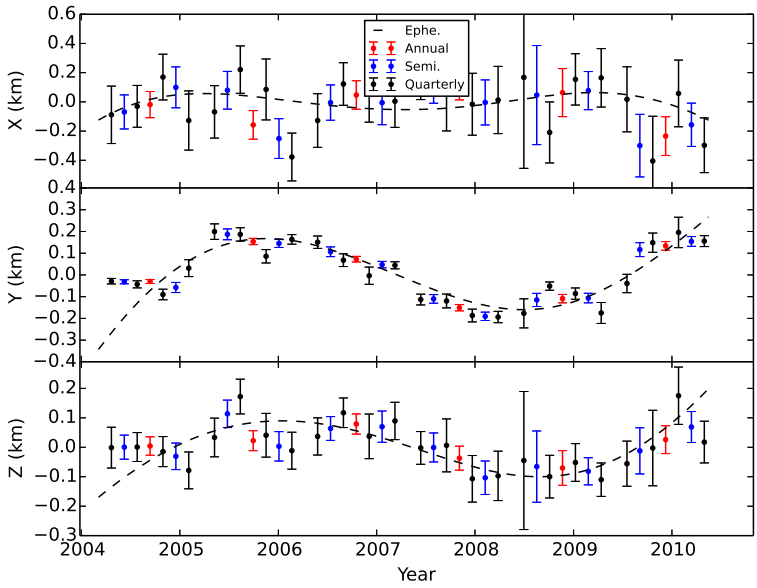

Fig. 3 The offset of the origin in DE200 compared to DE421. The red error bars, blue error bars and black error bars show the simulation results of annual, semi-annual and quarterly piecewise intervals respectively. The dashed lines show the actual differences in the vector from the Sun to the SSB between DE421 and DE200 after a quadratic term has been removed. The three panels are X, Y and Z components in the equatorial coordinate system.

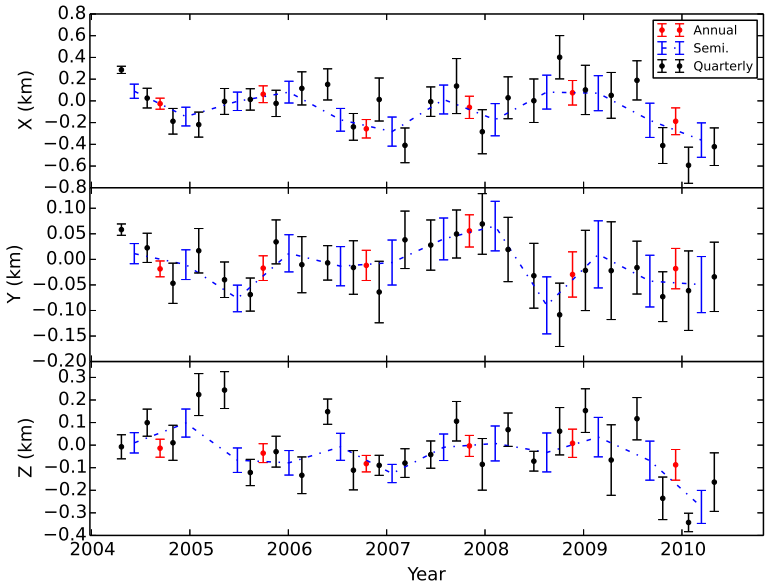

Fig. 4 The offset of the origin in DE421 with our data. The red error bars, blue error bars and black error bars show the results of annual, semi-annual and quarterly piecewise intervals respectively.

Figures 4 and 6 indicate that the results on the estimate of the offset of the origin in an ephemeris using different piecewise intervals and pulsar groups basically agree with each other. The trend and range in the reduction are approximately similar. The range of the offset of X, Y and Z components is at the level of several hundred meters, the same as the accuracy of the JPL DE series of ephemerides.

5 CONCLUSIONS

Based on the mathematical relation between the uncertainty of the vector from Earth to the SSB in the ephemeris and the timing residuals, we estimate the vector uncertainty by using observations of the most accurate pulsar timing data currently available. Since the quadratic term of the reduction is correlated with the rotation parameters of the

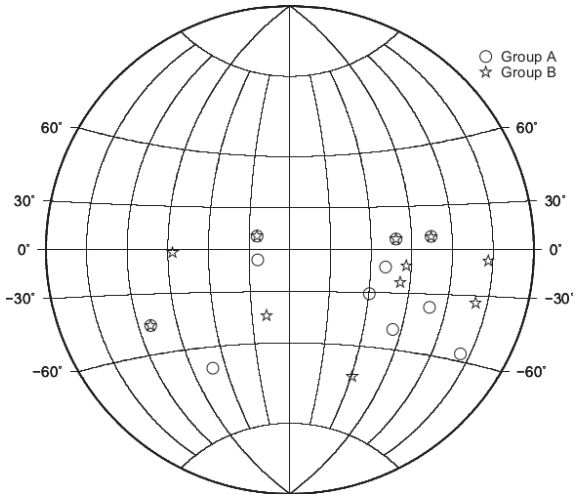

Fig. 5 The distribution of pulsars in different groups on the celestial sphere in the equatorial coordinate system.

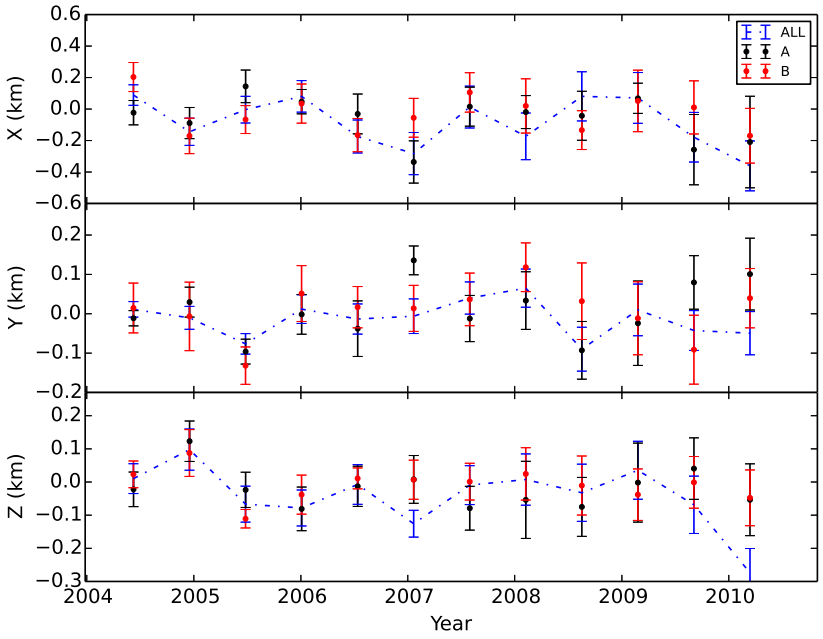

Fig. 6 The offset of the origin in DE421 using different groups of pulsars. 18 MSPs are represented by blue error bars, Group A is represented by black error bars and Group B is represented by red error bars.

pulsar and the annual term has a correlation with the position fits, the uncertainty of the vector from the Earth to the SSB is estimated after a quadratic term and annual term have been removed. We basically get similar results using different piecewise intervals of the data and pulsar groups. However, errors in the ephemerides, variations in the interstellar propagation path, intrinsic variations of pulsars and so on will introduce timing noise. A further study is needed to confirm how these factors affect the offset and what is the origin of the signal in the ephemeris.

Pulsar timing is a unique technology that is critical to the origin of a planetary ephemeris, and we can have a much better identification of the position of the SSB by pulsar timing. It will be helpful to improve the accuracy of pulsar-based navigation. With improvement in the observational accuracy and an extension of available timing data, it is likely that the uncertainty of the Earth-SSB vector in a planetary ephemeris will be estimated more accurately.

Acknowledgements The authors would like to thank G. Hobbs, Jing-Bo Wang and W. Coles for comments and suggestions. This work is supported by the National Natural Science Foundation of China (U1431117), and the Opening Project of Shanghai Key Laboratory of Space Navigation and Position Techniques (3912DZ227330001).

References

Champion, D. J., Hobbs, G. B., Manchester, R. N., et al. 2010, ApJ, 720, L201

Coles, W., Hobbs, G., Champion, D. J., Manchester, R. N., & Verbiest, J. P. W. 2011, MNRAS, 418, 561

Deng, X. P., Hobbs, G., You, X. P., et al. 2013, Advances in Space Research, 52, 1602

Edwards, R. T., Hobbs, G. B., & Manchester, R. N. 2006, MNRAS, 372, 1549

Fienga, A., Manche, H., Laskar, J., & Gastineau, M. 2008, A&A, 477, 315

Folkner, W. M., Williams, J. G., & Boggs, D. H. 2009, Interplanetary Network Progress Report, 178, C1

Hobbs, G. B., Edwards, R. T., & Manchester, R. N. 2006, MNRAS, 369, 655

Hobbs, G., Lyne, A. G., Kramer, M., Martin, C. E., & Jordan, C. 2004, MNRAS, 353, 1311

Hobbs, G., Archibald, A., Arzoumanian, Z., et al. 2010, Classical and Quantum Gravity, 27, 084013

Hotan, A. W., van Straten, W., & Manchester, R. N. 2004, PASA, 21, 302

Li, G.-Y., Ni, W.-T., & Tian, L.-L. 2003, Publications of Purple Mountain Observatory, 22, 73 (in Chinese)

Manchester, R. N., Hobbs, G. B., Teoh, A., & Hobbs, M. 2005, AJ, 129, 1993

Pitjeva, E. V. 2009, in Journées Systèmes de Référence Spatio-temporels 2008, ed. M. Soffel & N. Capitaine, 57

Schuh, H., & Behrend, D. 2012, Journal of Geodynamics, 61, 68

Standish, Jr., E. M. 1982, A&A, 114, 297

Verbiest, J. P. W., Bailes, M., van Straten, W., et al. 2008, ApJ, 679, 675

Verbiest, J. P. W., Bailes, M., Coles, W. A., et al. 2009, MNRAS, 400, 951

Wang, J. B., Hobbs, G., Coles, W., et al. 2015, MNRAS, 446, 1657